DESIGN OF A SWITCHED–RELUCTANCE MOTOR DRIVE FOR ELECTRIC PROPULSION

Second Annual Report – Part 2 (AR2.2)

An Enhanced Simple Method for Designing Switched Reluctance Motors Under Multi-Phase Excitation

Edilberto Mitre Hall, Shyam S. Ramamurthy, Juan Carlos Balda

University of Arkansas
Department of Electrical Engineering
3217 Bell Engineering Center
Fayetteville, AR 72701 – 1201
(501) 575-3005

Prepared for

June 2000

20000622 033

AN ENHANCED SIMPLE METHOD FOR DESIGNING SWITCHED RELUCTANCE MOTORS UNDER MULTI-PHASE EXCITATION

I.   INTRODUCTION

The Second Annual Report has been divided into three parts in order to summarize the activities performed on this ONR grant from May 1, 1999, until May 31, 2000. The three parts are the following:

- Part 1 entitled "Modeling Switched Reluctance Motors under Multi-Phase Excitation" covers "modeling" activities performed under Task (b) - "Design of the SRM" – of this ONR Grant.
- Part 2 entitled "An Enhanced Simple Method for Designing Switched Reluctance Motors under Multi-Phase Excitation" covers "design" activities performed under Task (b) - "Design of the SRM" – of this ONR Grant.
- Part 3 entitled "Modeling and Nonlinear Control of a Switched Reluctance Motors to Minimize Torque Ripple" covers "control" activities performed under Task (c) - "Design of the SRM Converter" – of this ONR Grant.

The reminder of this report refers to Part 2 of the Second Annual Report.

The Switched Reluctance Motor has been traditionally controlled using sequential single-phase excitation. Recently, several SRM configurations and control methods employing multi-phase excitation have been developed claiming performance improvements in terms of torque density, torque ripple, efficiency and acoustic noise [1-4]. The operation of these configurations under multi-phase excitation is described in terms of the phase inductances. This approach, though useful for understanding the operations of these configurations, cannot be used when designing the SRM. Unfortunately, the literature pertaining to these configurations does not include the procedure to design them, given a specification to be satisfied. When designing electric machines, one has to take into account the constraints imposed by the electric and magnetic loadings of the machine (i.e., current and flux densities, respectively).

This report shows a simplified method for designing SRMs under multi-phase excitation while taking into account the loading constraints imposed on the machine. The magnetic flux distributions, as obtained from ANSYS-based Finite Element Analysis (FEA), form the basis of the proposed method that extends the design equations in [5]. New design coefficients are obtained for the SRM operating under multi-phase excitation. The ideas are implemented in a computer program that calculates the main SRM dimensions, phase currents, copper losses and total weight. Descriptions of the design method and design program are included.

The SRM configurations considered are the 6/4 and 12/8 SRMs with short-, fractional- and full-pitch windings, and the 8/6 and 10/8 SRMs with short-pitch windings. For the same power rating, these most commonly used SRM configurations are designed to illustrate the method. Their performances in terms of magnetic loading and torque are then verified using FEA. A comparison of these configurations is included in terms of the main dimensions, weight, peak current and copper losses. The results illustrate that the perceived advantages of some configurations under multi-phase excitation are difficult to achieve when taking into account the constraints of the SRM magnetic loading.

II.   FEA ANALYSIS AND OPERATION OF DIFFERENT CONFIGURATIONS

This section evaluates the magnetic field distributions (obtained from the FEA analysis) and torque (by considering the linear (unsaturated machine) case and ideal current waveforms) of the considered SRM configurations. This analysis forms the basis of the design coefficients introduced in the next section.
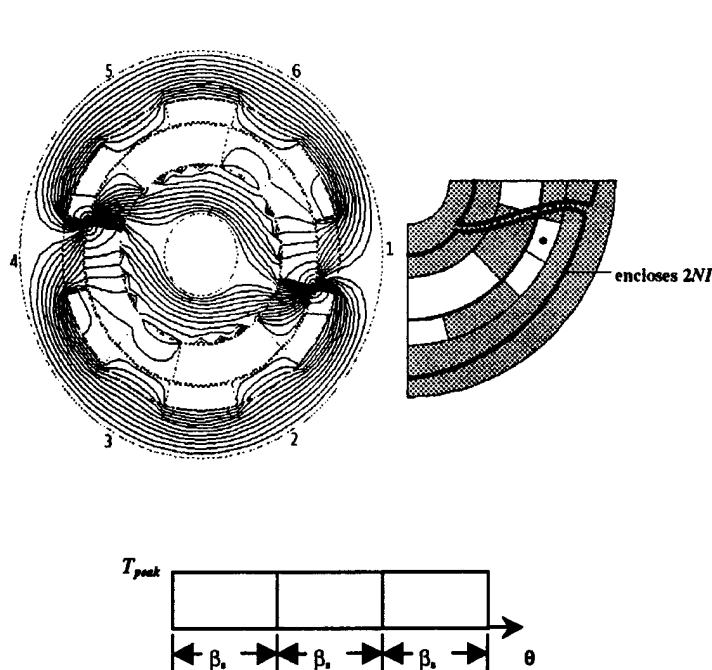
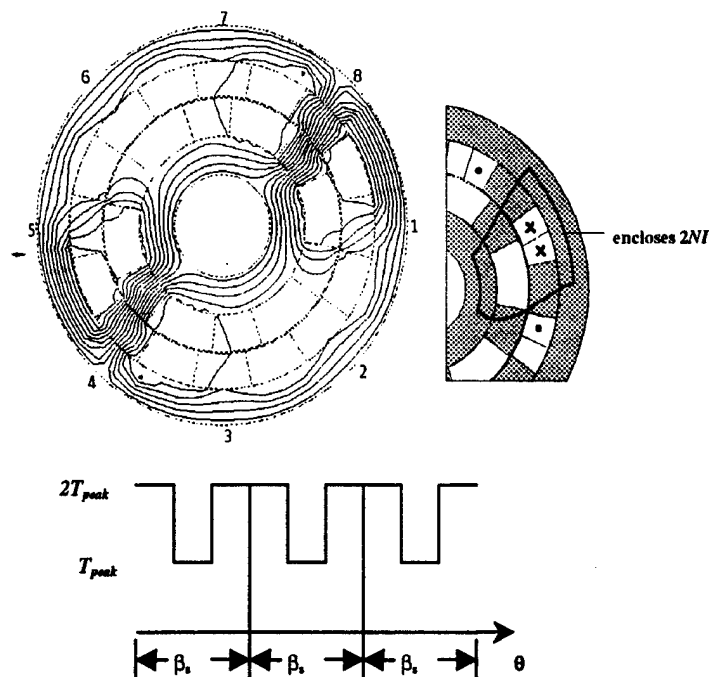Fig. 1 FEA plot, mmf diagram and the ideal
torque waveform for the 6/4 SRM.

Fig. 2 FEA plot, mmf diagram and the
ideal torque waveform for the 8/6 SRM.

A. Three-phase 6/4 SRM with short-pitch windings:

In SRMs with short-pitch windings, connecting the coils on physically opposing poles in series forms a phase. Only one phase is excited at a time to avoid negative torque components. Two phases only operate simultaneously during the commutation period where the current in the outgoing phase goes to zero and the current in the next incoming phase increases. Assuming that this commutation overlap is zero, the average torque of the machine is equal to T_{peak} in the unsaturated case. Fig. 1 shows the flux distribution in a 6/4 SRM with one phase excited.

Having $\beta_S = 30°$, the next incoming phase (e.g., the one formed by the coils on stator poles 1 and 4 in Fig. 1) starts to overlap with one pair of rotor poles at the time when the outgoing phase (in this case, the one formed by the coils on poles 3 and 6) has a complete overlap with the other rotor pole pair. The corresponding mmf diagram shows that the major flux path traverses the air-gap and returns through the back iron (i.e., a long flux path), and encloses a mmf of $2NI$. As a result, the mmf acting on a half path (of the major flux path) consisting of only one transversal through the air-gap is NI. Thus, this 6/4 SRM illustrates the simplest case of SRM operation, with only one phase and only one pole pair operating at a time to produce torque.

B. Four-phase 8/6 SRM with short-pitch windings:

The 8/6 SRM with short-pitch windings alternates between two-phase and one-phase operations. Fig. 2 shows the mmf diagram for the 8/6 SRM under two-phase excitation. Having $\beta_S = 22.5°$, a phase (e.g., the one formed by the coils on poles 1 and 5) can carry a current (to produce positive torque) simultaneously with the phase ahead of it (in this case, the one formed by the coils on poles 4 and 8) for the first 7.5° followed by single-phase operation for the next 7.5° and again, simultaneous conduction with the next incoming phase (formed by the coils on poles 2 and 6). The operation will alternate between long and short flux-path modes. The mmf acting on the major flux path indicated is $2NI$.
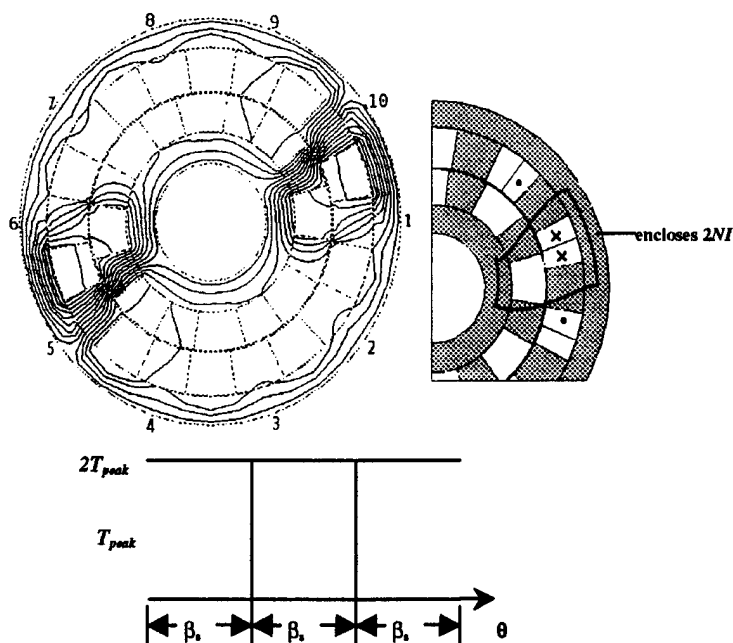
Fig. 3 FEA plot, mmf diagram and the ideal
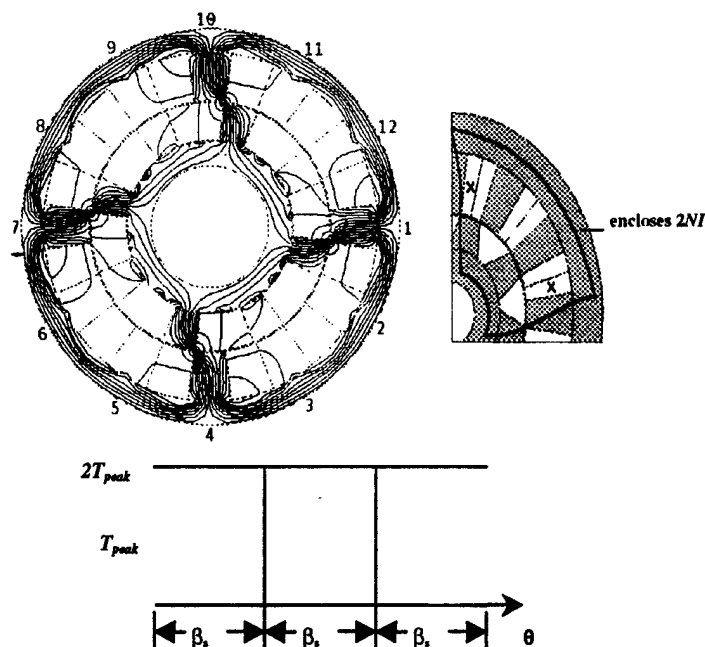torque waveform for the 10/8 SRM.

Fig. 4 FEA plot, mmf diagram and the ideal torque
waveform for the 12/8 SRM.

It is noted that the amount of flux returning through the back iron of the stator and the rotor in the long flux-path mode (i.e., one phase excited) is reduced as compared to the 6/4 SRM case. Even when two phases are excited, there is no increase in the mmf acting as compared to the single-phase operation case of the 6/4 SRM. With two phases excited, the major flux path will be a short flux path, if the winding polarities are chosen to achieve this as illustrated in the mmf diagram (i.e., it returns through a shorter length of the back iron instead of traversing the full length of the back iron which is the case of the long flux path). Short flux paths have smaller core losses than long flux paths. The torque in the ideal unsaturated machine will take the form shown in Fig 2.

The average torque developed in this case is $(3/2)\ T_{peak}$. It can be seen from Fig. 2 that two pairs of poles can participate simultaneously in torque production in the 8/6 SRM. The torque output is hence higher than that of the configuration in A.

C. Five-phase 10/8 SRM with short-pitch windings:

This SRM can operate continuously in the two-phase mode. From the mmf diagram in Fig. 3, the mmf acting over the major flux path (a short flux path) is $2NI$ and there is no increase in the mmf acting over a half path as compared to A. With $\beta_s = 18°$, a phase (e.g., the one formed by connecting the coils on poles 1 and 6) can carry current simultaneously with the phase ahead of it (in this case, the one formed by connecting the coils on poles 5 and 10) for 9° followed by simultaneous conduction with the next incoming phase (the one formed by connecting the coils on poles 2 and 7) for the next 9°. The torque for the ideal unsaturated machine takes the form shown in Fig. 3. During the commutation period, three phases conduct simultaneously. The average torque developed by the machine is $2T_{peak}$. The torque output is higher than in A and B.

D. Three-phase 12/8 SRM with short-pitch windings:

In the 12/8 SRM (see Fig. 4), two phases (e.g., the ones formed by connecting the coils on poles 1 and 7 in series and the coils on poles 4 and 10 in series) start and reach complete overlap with the rotor poles simultaneously. As a result, these two phases can be connected in series or in parallel to form one phase. Thus, there are only three phases instead of six in the 12/8 SRM.
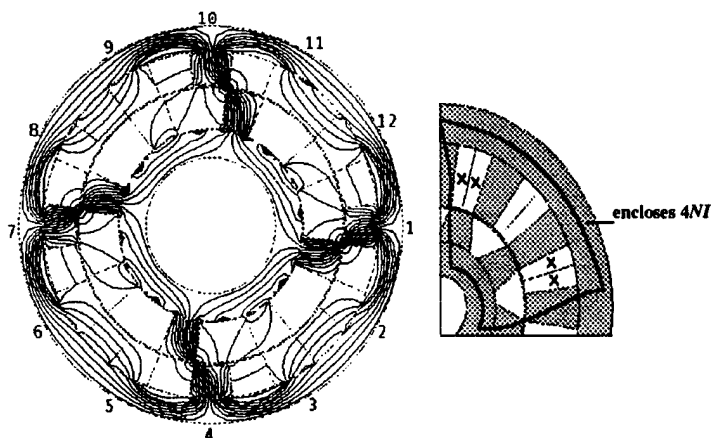
Fig. 5   FEA plot and mmf diagram for the
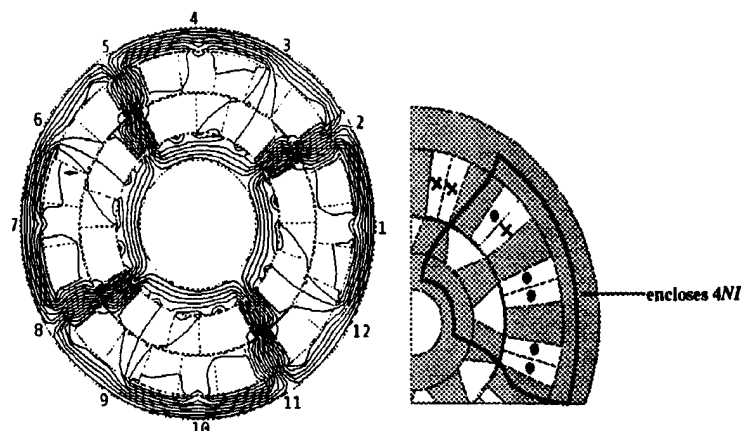12/8 SRM with full-pitch winding.

Fig. 6   FEA plot and mmf diagram for the 12/8 SRM with
fractional-pitch winding.

The mmf diagram of Fig. 4 shows that the major flux path encloses a mmf of $2NI$. The mmf acting over a half path remains the same as in A. The torque waveform takes the form shown in Fig. 4. The average torque is $2T_{peak}$, which is the same as in C.

E.   Three-phase 12/8 SRM with full-pitch windings:

The full-pitch winding is made up of coils whose sides occupy the entire available winding slot between poles. In the case of this 12/8 SRM shown in Fig. 5, coil sides lying between poles 1 and 12 and between poles 6 and 7 form a coil. Two such coils lying in winding slots in quadrature are connected in series or in parallel to form a phase. From the mmf diagram of Fig. 5, the mmf acting on a major flux path is $4NI$. Thus, the mmf acting over a half path is twice of those in A, B, C and D. Thus, the 12/8 SRM with full-pitch windings has increased mmf acting over the magnetic flux paths as compared to the 12/8 SRM with short-pitch windings. However, two phases have to be excited at all times. The torque waveform and output are the same as in C and D.

F.   Three-phase 12/8 SRM with fractional-pitch windings:

The coil sides in the 12/8 fractional-pitch windings occupy winding slots that are 120 electrical degrees away. A phase is formed by connecting four such coils in series. The mmf diagram in Fig. 6 shows that the mmf acting on a major flux path is $4NI$. The mmf acting over a half path is thus the same as that of E. The torque waveform is the same as that of cases C, D and E. This configuration also results in increased mmf acting over the magnetic flux paths as compared to the 12/8 SRM with short-pitch windings.

III.   DESIGN COEFFICIENTS FOR MULTI-PHASE OPERATION

Here, we introduce the coefficients enabling the design of the SRM under multi-phase excitation. These coefficients are useful for extending established design procedures on SRMs operating under single-phase excitation (such as the one described in [5]). It must be noted that some of the equations listed in [5] are only valid for the specific case of the 6/4 SRM under single-phase excitation.

It is well know that the SRM operates in a sequence of strokes; under single-phase excitation, each phase may conduct for a stroke angle given by:

$$\theta_{ST} = \frac{360}{mN_R}.$$

In some SRM configurations (e.g., the 8/6 and 10/8 SRM considered in this report), the stator-pole arc β_S is greater than the stroke angle. As a result, only the fraction θ_{ST}/β_S of the stator-pole width is actually utilized in torque-production under single-phase operation. To account for this, we introduce the stroke angle coefficient that is given by:

$$K_{ST} = \frac{\beta_s}{\theta_{ST}}$$

With this background, we present the equations for calculating the number of turns/pole N, the peak torque per pole pair T_{peak} (which is used for sizing the rotor dimensions [5]), the peak winding current I_{peak} and the rms winding current I_{rms}. While doing this, we will introduce other design coefficients.

A. *Number of turns/pole N:*

The magnetic flux per pole is given by

$$\Phi = \frac{B_s \, t_s \, L_{STK}}{k_{ST}}. \tag{1}$$

From (1) the flux linkage for two coils in series is given by:

$$\lambda = 2 \, N \, \Phi . \tag{2}$$

The DC voltage V_{DC} required to produce the magnetic flux in the core is calculated as follows [5]:

$$V_{DC} = (d\lambda / d\theta) \, \omega = \left(\frac{\lambda}{\theta_{ST}} \right) \omega. \tag{3}$$

Substituting (1) and (2) into (3) and solving for the number of turns/pole N yields:

$$N = K_{ST} \times \frac{46500 \times V_{DC}}{rpm \times m \times t_s \times L_{STK} \times N_R \times B_s}. \tag{4}$$

When the coils on more than one pole pair are connected in series to form a phase, (4) must be divided by $(P/2)$. The constant 46500 is due to the conversion of variables in the International System of Units (SI) to English units to be consistent with [5].

B. *Peak torque per pole pair T_{peak}:*

The average peak torque is related to the peak power and the rated speed ω at which the torque has to be developed as follows:

$$T_{avg \, .peak} = \frac{P_{peak}}{\omega}. \tag{5}$$

In the previous section, we noted that:

- Only one pair of poles develops torque at any given time in the 6/4 SRM, and
- The average torque developed in the 10/8 SRM is twice of that developed by that one pole pair.

Thus, for a given average peak torque, the peak torque to be developed by a pole pair in the 10/8 SRM is half of that to be developed by one pole pair in the 6/4 SRM. To account for this in the design equations, we introduce torque coefficient K_T that accounts for the reduction in torque to be developed by only one pole pair in a particular configuration. As per our definition, $K_T = 1$ for the 6/4 SRM and $K_T = 2$ for the 10/8 SRM.

Up to this point, we only considered the unsaturated operation of the SRM. However, the actual SRM operates under saturation. Thus, we introduce the coefficient K_{Tpeak} accounting for the effects of saturation and given as the ratio of the ideal peak torque to the average value obtained from FEA analysis; that is $K_{Tpeak} = T_{peak}/T_{avg}$.

In general, the average peak torque developed by the SRM is given by

$$T_{avg,peak} = \frac{K_T \times \dfrac{P}{2}}{K_{Tpeak} \times K_{ST}} \times T_{peak}. \tag{6}$$

From (5) and (6), the peak torque to be developed by only one pole pair is given by:

$$T_{peak} = \frac{K_{Tpeak} \times K_{ST}}{K_T \times \dfrac{P}{2}} \times \frac{P_{peak}}{\omega}. \tag{7}$$

C. Peak winding current I_{peak}:

In a 6/4 SRM with short-pitch windings under single-phase excitation, the peak winding current for developing the torque T_{peak} with only one pole pair is given by [5]:

$$I_{peak} = \frac{T_{peak}}{N \times B_S \times D_R \times L_{STK}}. \tag{8}$$

In SRM with full- and fractional-pitch windings, the winding arrangement results in increased mmf acting on the flux paths. As a result, the winding current can be reduced for a desired flux density to be developed in the air-gap. To account for this, we introduce the coefficient K_I which is the amount by which the winding current can be reduced as compared to the short-pitch winding case. By this definition, $K_I = 1$ in the 6/4 and 8/6 SRM, and $K_I = 2$ in the 12/8 SRM with fractional- or full-pitch windings. Thus, the peak winding current can be calculated as:

$$I_{peak} = \frac{1}{K_I} \times \frac{T_{peak}}{N \times B_S \times D_R \times L_{STK}}. \tag{9}$$

This equation applies when the coils on the pole pairs of a phase are connected in series. For the coil parallel connection, (9) should be multiplied by $(P/2)$.

In summary, we can calculate the turns/pole N, the peak torque to be developed by only one pole pair T_{peak} and the peak winding current I_{peak} using the new coefficients to modify the equations of the design procedure in [5]. For sizing the winding conductors, we need to calculate the rms value of the winding current I_{rms} as shown below.

D.   RMS winding current I_{rms}:

We introduce the coefficient K_A defined as the ratio between the rms and peak winding currents. This coefficient takes different values depending on the number of phase currents applied at any one time and the SRM configuration. For continuous single-phase operation, this ratio is given by [5]:

$$K_A = \sqrt{\frac{1}{m}}$$

(10)

since there is a current in only one phase for the duration of the stroke angle θ_{ST}. In the 8/6 and 10/8 SRMs under multi-phase excitation, the current pulse exists for the duration of the stator-pole arc β_s. This increase in conduction (and hence, the rms winding current value) can be accounted for by introducing the coefficient K_{ST} in (10). For example, $\beta_S = 18°$, $\theta_{ST} = 9°$ in the 10/8 SRM so the period of the current pulse is increased by a factor of $18/9 = 2$. Likewise, $\beta_S = 22.5°$ and $\theta_{ST} = 15°$ in the case of the 8/6 SRM with short-pitch windings under multi-phase excitation; the period of the current pulse increases by a factor of $22.5/15 = 1.5$.

Thus, in general for SRM with short-pitch windings:

$$K_A = \sqrt{\frac{K_{ST}}{m}}$$

(11)

In the full- and fractional-pitch winding SRM, K_A is given by the square root of the ratio of the number of phases conducting at a time and the total number of phases. For the three-phase full-pitch winding SRM having two phases conducting at any time, $K_A = \sqrt{\frac{2}{3}}$. For the three-phase fractional-pitch winding SRM, all three phases conduct at any given time and $K_A = \sqrt{\frac{3}{3}} = 1$.

The multi-phase design coefficients introduced in this section are listed in Table 1 for the considered SRM configurations.

Table 1. Design coefficients.

N_S / N_R	Winding Scheme	K_T	K_{ST}	K_I	K_A
6/4 or 12/8	Short pitch	1.0	1.0	1.0	0.5778
6/4 or 12/8	Full pitch	1.0	1.0	2.0	0.8165
6/4 or 12/8	Fractional pitch	1.0	1.0	2.0	1.0000
8/6	Short pitch, short flux path	1.5	1.5	1.0	0.6124
10/8	Short pitch, short flux path	2.0	2.0	1.0	0.6324

IV.   THE PROPOSED METHOD FOR SRM DESIGN AND RESULTS

Using the above design coefficients, a simple method for designing SRM under multi-phase excitation was developed. The method ideas were incorporated into a computer program that calculates the SRM main dimensions, peak current, total weight and winding losses given the input specifications. Fig. 7 shows the program flowchart.

The shaft diameter D_{shaft} is compared with the minimum $D_{shaft, min}$ value as given by ANSI [6]. The design provides space for the windings by considering a slot-fill factor of $K_S = 33\%$. The winding conductors are sized based on the continuous power rating of the SRM using AWG standard conductors.

Using the proposed design method, those SRM configurations shown in Table 2 under single- and multi-phase excitations were designed for the following specifications of an electric propulsion application:

DC Supply Voltage	= 300 V
Peak Power Rating	= 35 kW
Continuous Power Rating	= 23 kW
Rated Speed	= 1200 rpm
Maximum Speed	= 6000 rpm.

For different designs, Table 2 lists the stator outer radius and stack length, weight, peak winding current and copper losses. These results are obtained using the same constraints on maximum flux and current densities for all configurations. In the case of the 6/4 SRM with short-pitch windings under single-phase excitation, only one pole pair produces torque at a time. As a result, the rotor torque density is lower than in the 12/8 SRM with short-pitch windings under single-phase excitation where two pole pairs participate in torque production.
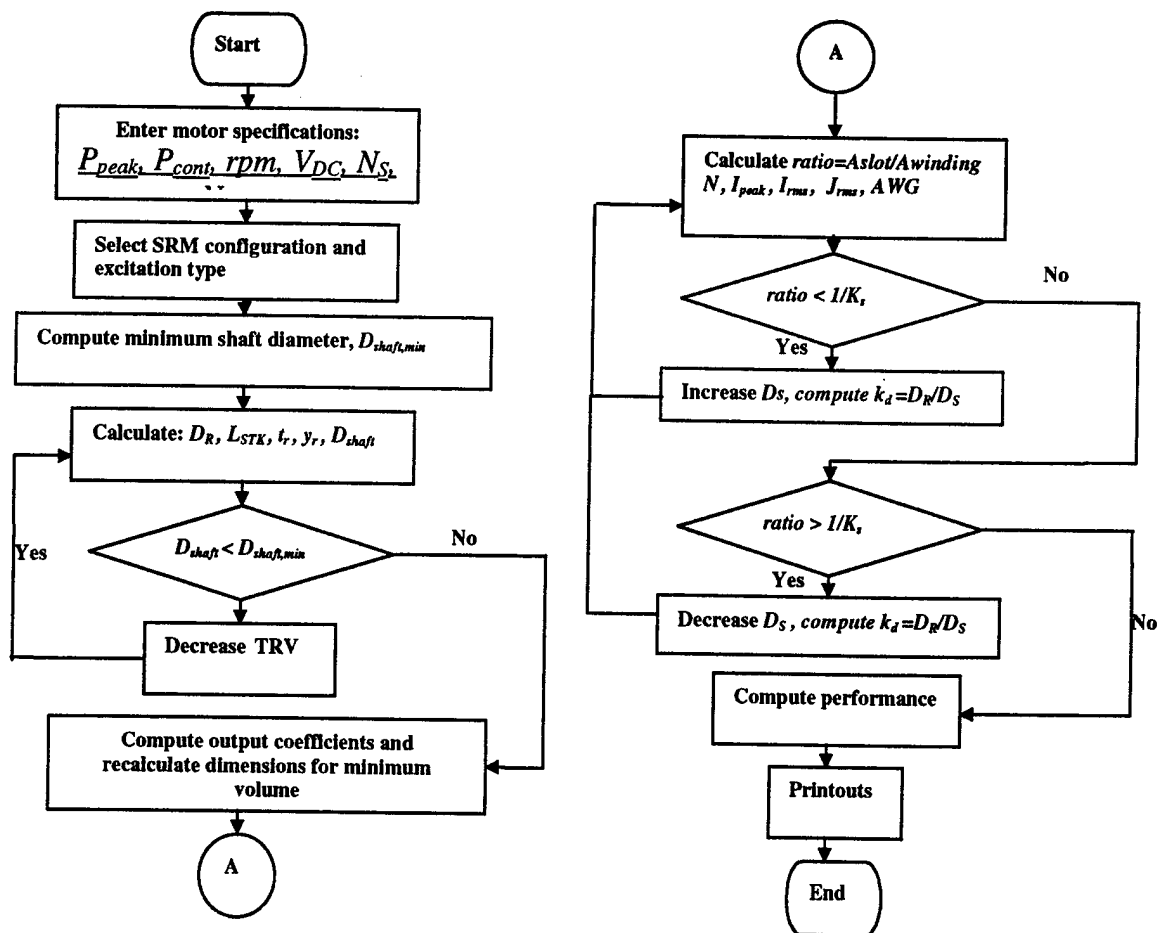

Fig. 7 Flowchart of the computer program that calculates the SRM main dimensions, peak current, total weight and winding.

Table 2. Design results.

N_S / N_R	Winding Scheme	Excitation Type	Stator Outer Radius (m)	Stack Length (m)	Weight (kg)	Peak Current (A)	Copper Losses @ P_{cont} (Watts)
6/4	Short pitch	Single phase	0.232	0.298	306	258	665
12/8			0.188	0.237	133	264	646
12/8	Full pitch	Multi phase	0.172	0.237	111	274	773
12/8	Fractional pitch	Multi phase	0.179	0.237	120	274	802
8/6	Short pitch	Multi phase (short flux path)	0.185	0.237	145	132	563
10/8			0.186	0.237	139	132	688

This can be seen as higher dimensions and weight for the 6/4 SRM as compared to the other configurations. Multi-phase operation of the 12/8 SRM using full- or fractional-pitch windings produces only a slight reduction in dimensions and weight. This is due to the higher rms winding current values for these configurations. Though the peak winding current can be reduced if the winding voltage is kept at same value as in the short-pitch winding SRM, the rms winding current, which determines the conductor size, approaches that of the 12/8 SRM with short-pitch windings. We have considered bipolar converters for the full- and fractional-pitch winding SRM so that the winding voltage is only 150 V as compared to a winding voltage of 300 V for the SRM with short-pitch windings. The peak current thus remains unchanged. The 8/6 and 10/8 SRM have comparable dimensions and weight to the 12/8 SRM.

V.   CONCLUSIONS

This report has presented a simple method for designing SRM operating under multi-phase excitation. This SRM design method takes into account the practical machine constraints very easily and can be simply implemented as an enhancement to existing design methods. The design results show that an improvement in torque density is obtained in those configurations that increase the number of pole pairs participating in the torque production. To this end, the full- and fractional-pitch windings do not change the number of pole pairs participating in torque production. Also, it is not possible to improve the torque density substantially by using full- and fractional-pitch windings due to the thermal constraints imposed by the maximum flux density. The apparent advantage of a better utilization of the winding area in the full- and fractional-pitch SRM is reduced by the higher value of K_A for these configurations. The short-pitch SRM use unipolar converters and the voltage applied across the windings is 300 V. The full- and fractional-pitch SRM may use bipolar converters but the voltage applied across each winding is only 150 V for star-connected windings (i.e., half of the DC bus voltage). The peak current for the converter switches remains unchanged. The choice of a particular SRM configuration should be also based on other factors such as high-speed operation, use of readily available standard inverters, ease of manufacturing, requirement of low torque ripple using current profiling between phases, noise-reduction needs and system losses.

VI.   REFERENCES

[1] A. Michaelides and C.Pollock, " Short Flux Paths Optimize the Efficiency of a 5-Phase Switched Reluctance Drive", *Conference Proceedings of the 1995 Annual Meeting of the IEEE Industry Applications Society*, pp.286-293.

[2] B.C. Mecrow, "New Winding Configurations for Doubly Salient Reluctance Machines", *IEEE Transactions on Industry Applications*, Vol. 32, No. 6, November-December 1996, pp. 1348-1356.

[3] Y. Tang, "Switched Reluctance Motor with Fractionally Pitched Windings and Bipolar Currents", *Conference Proceedings of the 1998 Annual Meeting of the IEEE Industry Applications Society*, pp. 351-358.

[4] J. Moon, S. Oh, J. Ahn and Y. Hwang, " Switched Reluctance Motor with 2-Phase Excitation", *Conference Proceedings of the 1998 Annual Meeting of the IEEE Industry Applications Society*, pp. 547-552.

[5] T.J.E. Miller, <u>Switched Reluctance Motor and Their Control</u>, Magna Physics Publishing and Clarendon Press – Oxford, 1993.

[6] E. Levi, <u>Polyphase Motors: A Direct Approach to Their Design</u>, John Wiley & Sons, 1984.

VII. NOMENCLATURE

B_S	Saturation flux density
D_R, D_S, D_{shaft}	Rotor, stator and shaft diameters
L_{STK}	Stack length
t_R, t_S	Rotor and stator-pole widths
y_r	Rotor yoke thickness
k_d	Ratio of rotor to stator diameter
K_S	Slot-fill factor
T_{peak}	Peak torque produced by a pole pair
$T_{avg,peak}$	Average peak torque developed by the SRM
P_{peak}	Peak power
N	Number of turn/pole
N_R, N_S	Number of rotor and stator poles
m	Number of phases
P	Number of pole pairs/phase $= N_s / m$
rpm, ω	Rated speed in rev/min and rad/sec
I, J	Current and current density
V, E	Voltage and electromotive force
θ_e, θ_m, θ_{ST}	Electrical, mechanical and stroke angles
β_R, β_S	Rotor- and stator-pole arcs
TRV	Torque per unit rotor volume

Subscripts avg, mech, cont, rms, I, DC, T, ST, min, STK denote average, mechanical, continuous, effective value, current, direct current, torque, stroke, minimum, and stack, respectively.

REPORT DOCUMENTATION PAGE

1. AGENCY USE ONLY *(Leave blank)*	2. REPORT DATE	3. REPORT TYPE AND DATES COVERED
	June 2000	Annual Report, 5/1/99 to 5/30/00 (Pt.2)

4. TITLE AND SUBTITLE
Second Annual Report - Part 2 (AR2.2)
An Enhanced Simple Method for Designing Switched
Reluctance Motors under Multi-Phase Excitation

5. FUNDING NUMBERS
G 00014-98-1-0617
PR 98PRO5665-00

6. AUTHOR(S)
Edilberto Mitre Hall, Shyam S. Ramamurthy,
Juan Carlos Balda

7. PERFORMING ORGANIZATION NAMES(S) AND ADDRESS(ES)
University of Arkansas, Office of Research and
Sponsored Programs, 120 Ozark Hall, Fayetteville,
AR 72701

8. PERFORMING ORGANIZATION REPORT NUMBER
AR2.2

9. SPONSORING / MONITORING AGENCY NAMES(S) AND ADDRESS(ES)
Office of Naval Research
ONR 242
Ballston Centre Tower One, 800 North Quincy Street
Arlington VA 22217-5660

10. SPONSORING / MONITORING AGENCY REPORT NUMBER

11. SUPPLEMENTARY NOTES

a. DISTRIBUTION / AVAILABILITY STATEMENT
APPROVED FOR PUBLIC RELEASE

12. DISTRIBUTION CODE

13. ABSTRACT *(Maximum 200 words)*
Part 2 of 3 of the Second Annual Report covers "design" activities performed under Task (b) - "Design of the SRM" of this ONR Grant. The activities were performed from 5/1/99 to 5/30/00. This report shows a simplified method for designing switched reluctance motors (SRM) under multi-phase excitation while taking into account the loading constraints imposed on the machine. The SRM configurations considered are the 6/4 and 12/8 SRM with short-, fractional- and full-pitch windings, and the 8/6 and 10/8 SRM with short-pitch windings. The results illustrate that the perceived advantages of some configurations under multi-phase excitation are difficult to achieve when taking into account the constraints of the SRM magnetic loading.

14. SUBJECT TERMS
Annual report, main activities.

15. NUMBER OF PAGES
11

16. PRICE CODE

17. SECURITY CLASSIFICATION OF REPORT	18. SECURITY CLASSIFICATION OF THIS PAGE	19. SECURITY CLASSIFICATION OF ABSTRACT	20. LIMITATION OF ABSTRACT
UNCLASSIFIED	UNCLASSIFIED	UNCLASSIFIED	UL